15. STABILITY AND THERMAL ANALYSIS

15.1 INTRODUCTORY CONSIDERATIONS

The main topic of this chapter is *stability*. In this case the term *stability* means, the ability of the coil to support local or distributed temperature rises above the nominal temperature without quenching. Before giving details, it is important to define some important parameters to prevent misunderstanding.

The critical temperature, with no current flowing in the conductor, T_c, only depends on the magnetic field. For NbTi the critical temperature is according to:

$$T_c(B) = T_{c0}\left(1 - \frac{B}{B_{c\,20}}\right)^{0.59}, \qquad (15.1)$$

where T_{c0} is the critical temperature at B = 0 (T_{c0} = 9.3 K), and B_{c20} is the critical field at T = 0 (B_{c20} = 13.9 T). At B = 4.6 T, the CMS peak field, T_c = 7.35 K. Considering that a current I_0 flows in the conductor, a new critical temperature T_{cs} is defined as the maximum temperature for which the current I_0 can flow with no dissipation in the superconducting part. T_{cs} is called the current sharing temperature.

$$T_{cs} = T_c - (T_c - T_0)\frac{I_0}{I_c(T_0, B)}, \qquad (15.2)$$

where $I_c(T_0, B)$ is the critical current at nominal temperature and peak field. For CMS, T_{cs} has been fixed at 6.5 K, allowing the magnet to operate at 1/3 of the critical current.

In order to organise the concepts related to the stability, three cases of heat dissipation inside the coil may be distinguished:

a) A fixed amount of energy E_0 is released as heat inside the winding (localised or also distributed) in a given time, t_0, in such a way that the temperature rise in the winding will not be higher than $T_{max} < T_{cs}$.
b) A steady state power dissipation occurs inside the winding. The heat is drained away by the LHe coolant, through the thermal conductance of the cold mass, in such a way that the maximum temperature does not exceed T_{cs}.
c) A fixed amount of the energy E_0 is locally released as heat inside the winding in a given time, t_0, causing a local increase of temperature over the critical temperature $T_{max} > T_{cs}$.

It is possible to find for each case the conditions at which the coil can operate without quenching.

For case a) we can define the maximum energy for unit volume $E_{u.v}$ causing a temperature rise within T_{cs}. $E_{u.v}$ is related to the distributed heat released in large volumes (up to the complete coil). For a safe design the value of $E_{u.v}$ should be as high as possible. The question is *how large should $E_{u.v}$ be ?* or in other words *what is the reference energy to be compared with $E_{u.v}$?* There are two possible answers to this question:

a) $E_{u.v}$ should be compared with values of existing running coils of the same kind;
b) An analysis should be carried out in order to evaluate the reasons leading to energy releases in a large fraction of the coil.

These points are addressed in section 15.2, which discusses all these topics grouped together in a single subject called Enthalpy Margin.

In case b) there are steady heat inputs to a given zone of the coil, due to several reasons such as a conductor joint, eddy currents during charging and discharging or heat conduction through the supports. The heat is drained away by the cooling system through the conductance of the cold mass and a temperature gradient results inside the cold mass. The aim of the design is to have a cold mass conductance (in every direction) and a cooling capacity so high that reasonable heat sources can only cause negligible temperature rises (not higher than 50 mK). These topics are more related to the cooling system and are not discussed in this chapter.

In case c) we analyse the situations for which localised quenches occur. The aim of the analysis is to understand the conditions needed to restore to a fully superconducting state, ($T < T_{cs}$). In principle it should only be necessary to answer the following three questions:

a) Does a threshold value of localised disturbance energy exist, for which the local transition grows (quenching the coil) or recovers ?
b) What is the definition of a localised disturbance? What happens for distributed disturbances?
c) What are the possible sources of the disturbances?

These topics, which are related to concepts such as Minimum Quench Energy and Minimum Propagating Zone, constitute the main part of the stability chapter and are discussed in sections 15.3, 15.4, and 15.5.

15.2 ENTHALPY MARGIN

As was discussed in the previous section the current can flow with no dissipation in the superconducting cross section up to a temperature of 6.5 K. In the temperature range 6.5 K - 7.34 K, the current is shared between the superconductor and the matrix. Fig. 15.1 shows the critical current scales for field and temperature. The load line of the peak field intercepts the critical curve $I_c(B)$ at 20 kA for a temperature of 6.5 K. An interesting parameter is the enthalpy variation from 4.5 K to 6.5 K:

$$E_{u.v.} = \int_{4.5}^{6.5} Cp(T)\delta dT, \quad (15.3)$$

where Cp(T) is the specific heat (in J/Kg) and d the density. By averaging the thermal properties among the four parts of the winding (Aluminium, Copper, NbTi and fibreglass epoxy), we find $E_{u.v.}$ = 2550 J/m^3. This enthalpy margin can be re-written in a more convenient way as energy per unit conductor length, resulting in $E_{u.l.}$ = 4.2 J/m. About 50% of the enthalpy margin is provided by the structural material (Aluminium alloy) tightly coupled to the conductor.

As stressed in the previous section, the aim of the design consists in maximising the enthalpy margin. At a fixed magnetic field, the only way to increase the margin is to increase the superconducting cross section. It is interesting to graph the enthalpy margin as a function of the superconducting cross section as shown in Fig. 15.2. The maximum margin is 3890 J/m^3, corresponding to T_{cs} = 7.35 K, requiring an infinite superconducting cross section. The actual choice of 22.3 mm^2, gives a margin of 2550 J/m^3 (65% of the ideal maximum one) and can be considered a good compromise. As an exercise, doubling the present cross section will increase the margin to 3200 J/m^3. Unfortunately this modest growth (25% more) has a big impact on the conductor cost.

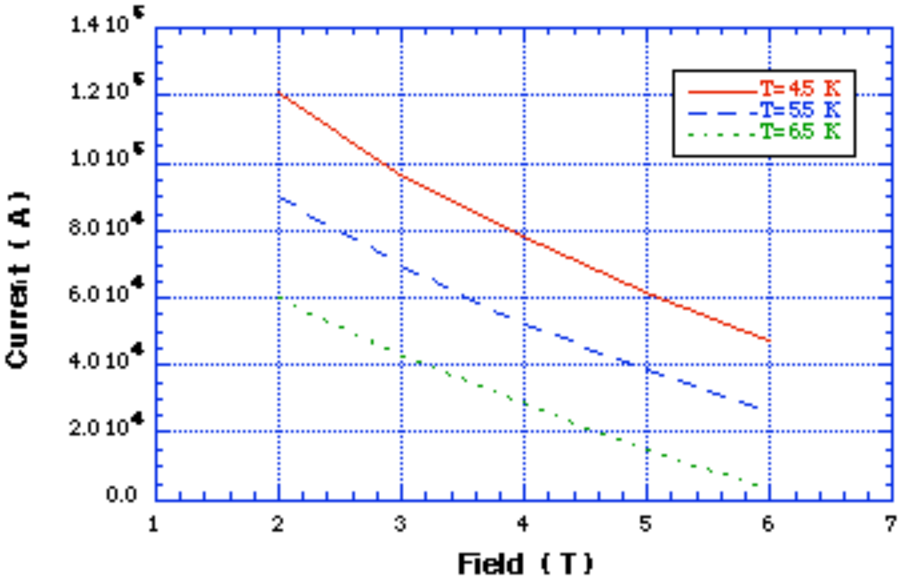

Fig. 15.1: Critical current Vs magnetic field at 3 different temperatures, intercepting the peak field load line.

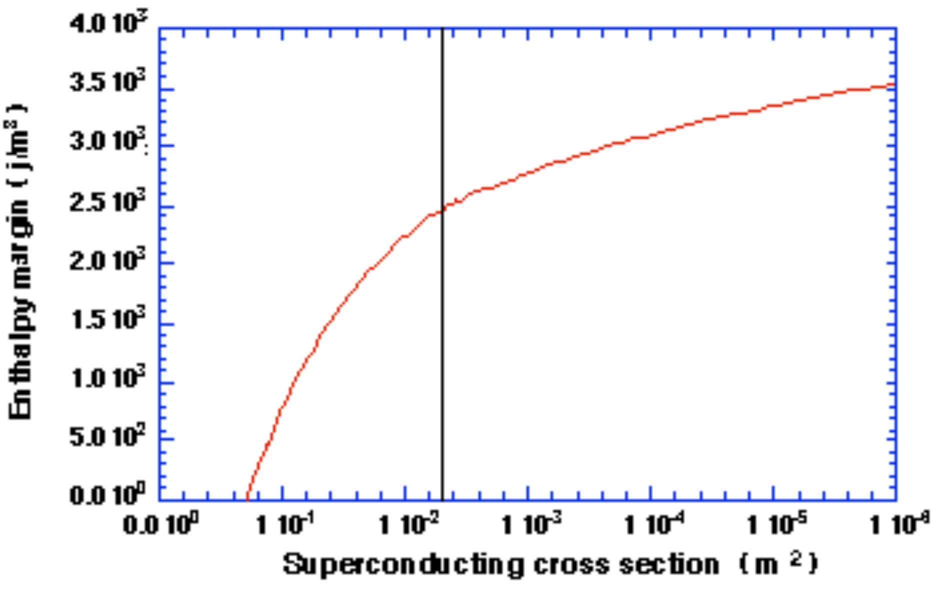

Fig. 15.2: Enthalpy margin Vs the superconducting cross section.

In the introduction section it was stated that in order to understand how large is the enthalpy margin, it is useful to perform comparisons with existing running coils of the same kind. For this comparison we chose the superconducting thin solenoids of the CDF and ALEPH experiments. CDF was chosen as a reference coil because it is one of the oldest thin solenoids of large dimensions still working today. Furthermore it is particularly critical from the stability point of view. ALEPH is the biggest existing thin solenoid and its design is particularly well known to the CMS design team. The parameters of interest for stability computations are shown in Table 15.1. Using that data the enthalpy margin for ALEPH and CDF is calculated to be respectively 2800 J/m^3 and 1300 J/m^3. In terms of energy per unit length we have respectively 0.4 J/m and 0.1 J/m. It is clear that from the point of view of any disturbance directly released inside the conductor or close to it, the energy per unit length is more significant.

Under this view, the CMS conductor could seem to be much more stable due to its large cross section: we have a factor of 10 with respect to ALEPH and 35 with respect to CDF. Unfortunately the larger margin of the CMS coil with respect to ALEPH and CDF, does not necessarily mean higher stability, because we have not yet compared the margin with the disturbance sources in the cold mass of the three coils. Section 15.4 is devoted to such considerations, involving the disturbance spectrum in large Al-stabilised and indirectly cooled superconducting coils.

Table 15.1

Parameters used for stability computation on CMS, ALEPH and CDF coils.

Parameters	CMS	ALEPH	CDF
Layers	4	1	1
Conductor width (mm)	22.3	3.6	3.89
Conductor thickness (mm)	72	35	20
Turn/turn insulation(mm)	0.27	0.27	0.2
Cylinder thickness (mm)	12	50.0	16.0
Ground plane insulation (mm)	0.94	0.6	1
Bath temperature (K)	4.5	4.4	4.5
Peak field (T)	4.6	2.0	2.5
Nominal current (A)	20000	5000	5000
I/Ic	30%	40%	60%
Sharing temperature (K)	6.5	6.8	5.8
Critical temperature (K)	7.35	8.5	8.2
Current density in the Al matrix			
(A/mm^2)	28	40	64

15.3 TRANSIENT ANALYSIS. LOCALISED DISTURBANCES

In this section we will study the effects of perturbations causing localised transition to normal state ($T > T_{cs}$). In general it is supposed that a time dependent disturbance G(t) is released as heat inside the winding. In that zone, the critical temperature is exceeded causing a dissipation, $\dot{Q}(t)$, which depends on how much current is transferred from the superconductor to the aluminium matrix and also how the current is shared by the superconductor and the aluminium. From a mathematical point of view this situation can be studied by solving the heat transient diffusion equation by numerical methods The approach to the problem consists in imposing a given disturbance and solving the equation describing how the normal zone (if any) increases, causing a quench, or reduces, restoring full superconducting state.

The heat dissipation

When the temperature T is higher than the sharing temperature T_{cs}, the current is transferred to the matrix, causing a dissipation of unit volume:

$$\dot{Q} = \rho_{eff} J^2, \quad (15.4)$$

where r_{eff} is essentially the resistivity of the pure aluminium matrix, and J is the current density in the same metal. The current I_{Al} flowing through the aluminium depends on temperature: at $T = T_{cs}$, $I_{al} = 0$, at $T = T_c$, $I_{Al} = I_0$ (i.e. all the current). Eq. 15.4 is based on the assumption that the excess current in the superconductor can be immediately shared by the whole aluminium matrix. Unfortunately this assumption does not reflect the real situation occurring in a large Al-stabilised conductor. The current cannot be shared instantaneously by the aluminium matrix because of the eddy currents. The most appropriate description is given in terms of a diffusion of the electrical field according to the equation:

$$\Delta\vec{E} = \frac{\mu_0}{\rho}\frac{\partial\vec{E}}{\partial t}, \quad (15.5)$$

The heat dissipation is strongly modified by (15.5). Since it is difficult to take into account at the same time both the current sharing effect and the current diffusion effect, we used a simplified model for the heat generation by assuming that the heat dissipation starts when the temperature exceeds $T_s = (T_{cs}+T_c)/2$. As an example Fig. 15.3 shows the heat generation versus time using a numerical solution (for this solution we used the standard general purpose F.E. code ANSYS rev. 5.2) for the CMS conductor. At a time of a few milliseconds after the transition ($T > T_s$) the current remains in the Rutherford cable, causing heat generation of up to 100 times higher than the computed value using (15.4).

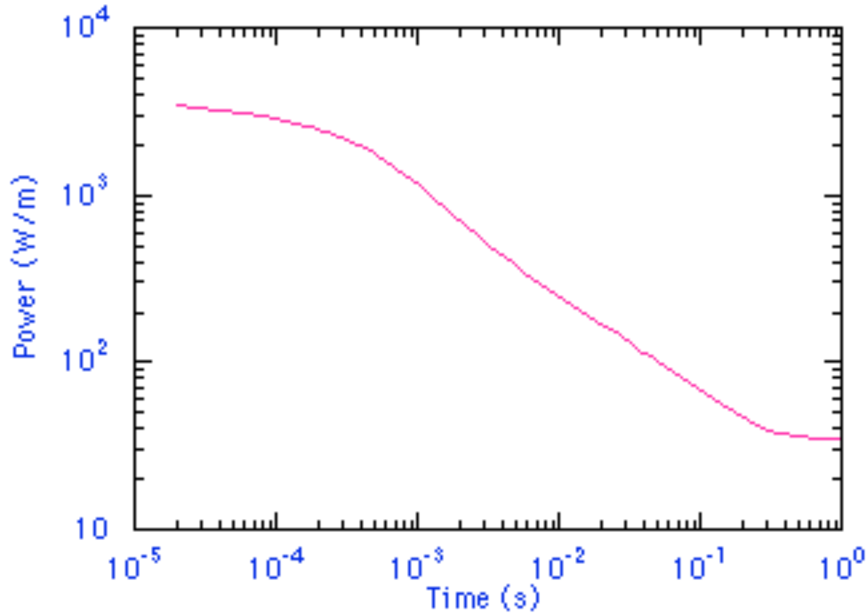

Fig. 15.3: Time dependent heat dissipation due to the current diffusion.

Approximately 1 second after the quench, the current in the Rutherford cable is close to being equally distributed in the whole aluminium cross section.

The disturbance

The disturbance is assumed to be a constant power dissipated for a given time in a given region. The time duration of the disturbance and the dimensions of the region where the energy is released are two very important parameters and will be discussed later.

Numerical solution of the heat conduction equation

The heat conduction equation was solved numerically by using a 3-D F.E. code for transient thermal problems (HEATING-7.2 developed at Oak Ridge National Laboratory). The code was implemented with a routine to compute the heat generation taking into account the effects of several parameters such as:

a) the material thermal and electrical properties as functions of field and temperature [electrical resistivity r = r (T, B), thermal conductivity k = k (T, B), specific heat C = C (T)],
b) the critical temperatures $T_{cs}(B, I_c)$ and $T_c(B)$,
c) the heat generation, including as an option, the current diffusion effect as expressed by (15.5).

Model for numerical computation

The winding is usually schematised as a solid parallelepiped, of which the plane X-Y represents a small portion of the Z-R cross section of the coil with a fixed number of adjacent turns. The longitudinal direction (Z) represents the coil azimuthal direction. The longitudinal length of the model should large enough that the results are not affected by changing this parameter (several meters are used).

The symmetry of the problem allows to use only a quarter of the model, cutting down the number of nodes and CPU time.

Figure 15.4 shows a cross section of the CMS winding model (plane X-Y corresponding to the plane Z-R of the coil) with 5 adjacent conductors for each layer, which the symmetry reduces to 2 and a half conductors. The four layers of the coil are represented. The thin supporting cylinder is not modelled for reasons explained later.

All the components of the winding (Rutherford, pure Al, Al alloy, insulation) are modelled. Since the localised disturbance is put in the central conductor of the first layer (at X = 0, Y = 0), only the first layer is completely modelled. For the remaining 3 layers the Rutherford cable and the aluminium stabiliser are grouped by averaging the electrical and thermal properties.

The system is assumed to be adiabatic with an initial temperature equal to the operating temperature (T_0 = 4.5 K).

The model was suitably meshed using parallelepiped elements. Each element is defined by 8 nodes. The total number of nodes ranges from 10000 to 17000. In order to use a reasonable CPU time, attention must be paid to minimising the number of the nodes. A model with 13000 nodes requires 46 h CPU time on a Digital ALPHA VAX to perform a transient analysis of 0.7 s.

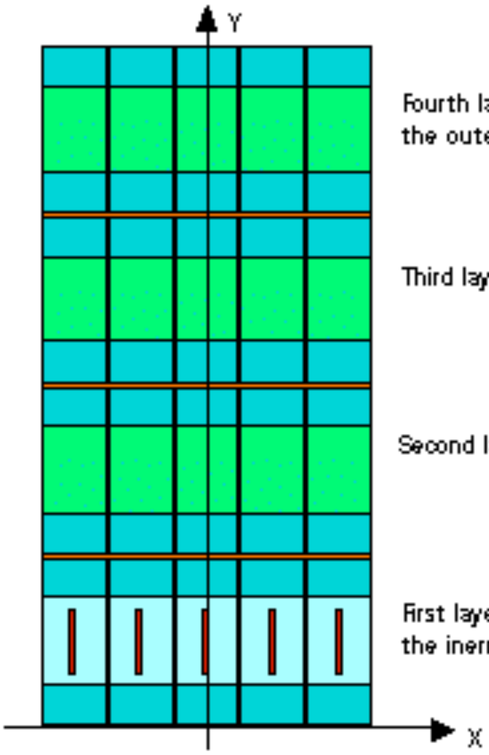

Fig. 15.4: Cross section (plane x-y equivalent to the z-r plane) of the CMS winding model.

Stability analysis

The analysis is carried out by imposing a disturbance and computing the time evolution of the temperature distribution. The disturbance is modelled by releasing a fixed amount of power for a given time in a given region. For CMS, as modelled in Fig. 15.4, the power was deposited in the central conductor (of 5) of the first layer, in a longitudinal length of 1 cm and for a time of 10 ms. A more complete discussion about the disturbance modelisation will be made in a later section.

The results can be usefully represented through a graph showing the quenched region in the longitudinal direction along the central conductor. In this case we assume normal zones to be the regions having temperature $T > T_s = (T_{cs}+T_c)/2$. Figs 15.5 and 15.6 show the time evolution of this transited length (with pure aluminium RRR = 800) in two different cases:

a) instantaneous current diffusion (Fig. 15.5),

b) finite current diffusion (Fig. 15.6) according to Eq. 15.5.

We showed the results for the Minimum Quench Energy for both cases because our model can be pessimistic when considering the current diffusion. In fact due to the difficulty to consider both the current sharing and the current diffusion effects, the transition to normal was schematised as a process occurring sharply at a temperature T_s intermediate between the sharing temperature T_{cs} and the critical temperature T_c. The simulations showed that large zones of the winding remain in the range T_{cs} to T_c. However the results obtained with instantaneous current diffusion give an upper limit to the stability.

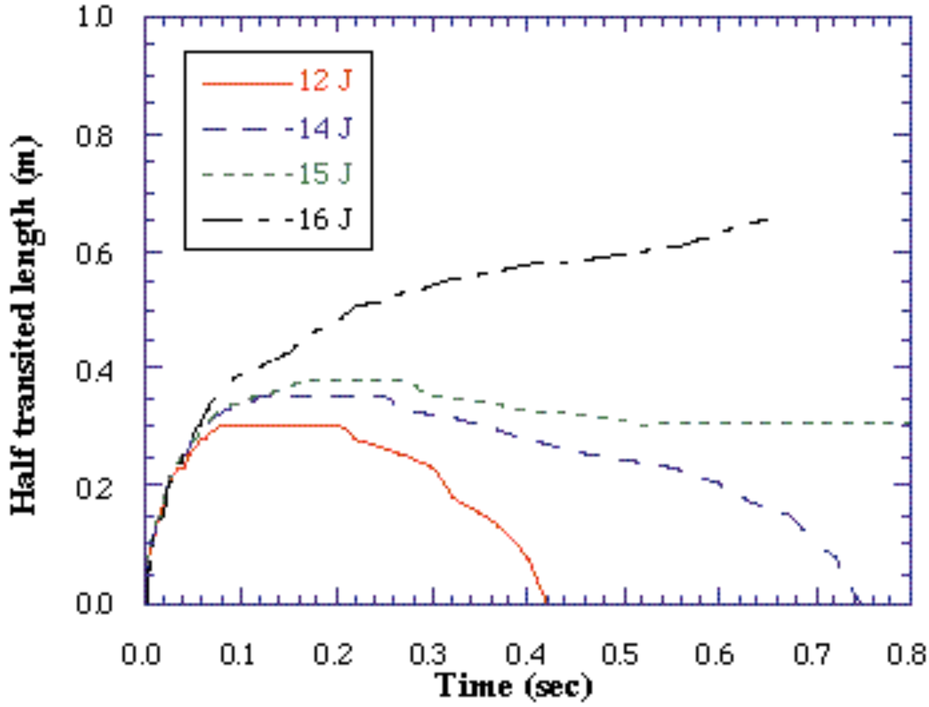

Fig. 15.5: Time evolution of the normal zone in the case of instantaneous current (and ideal) diffusion.

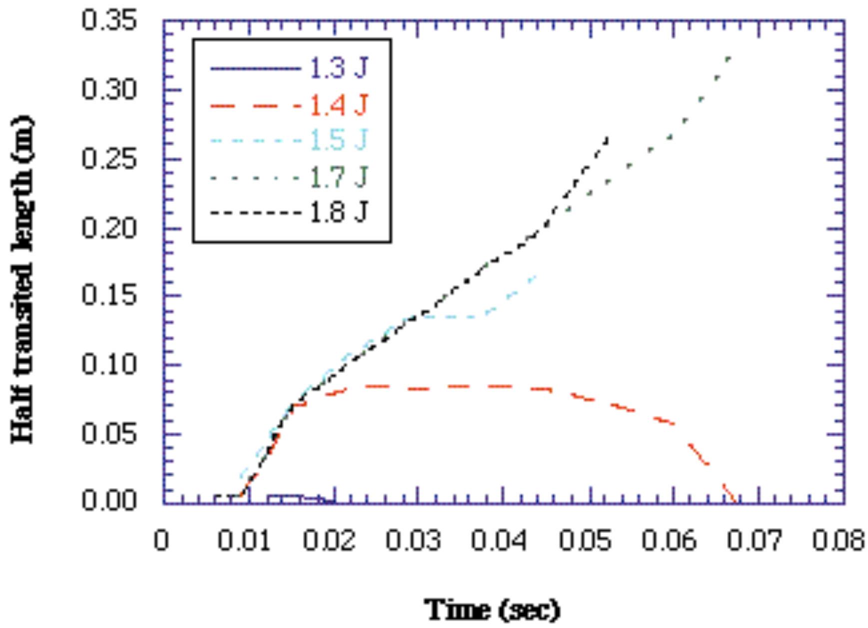

Fig. 15.6: Time evolution of the normal zone in the case of finite (and real) current diffusion.

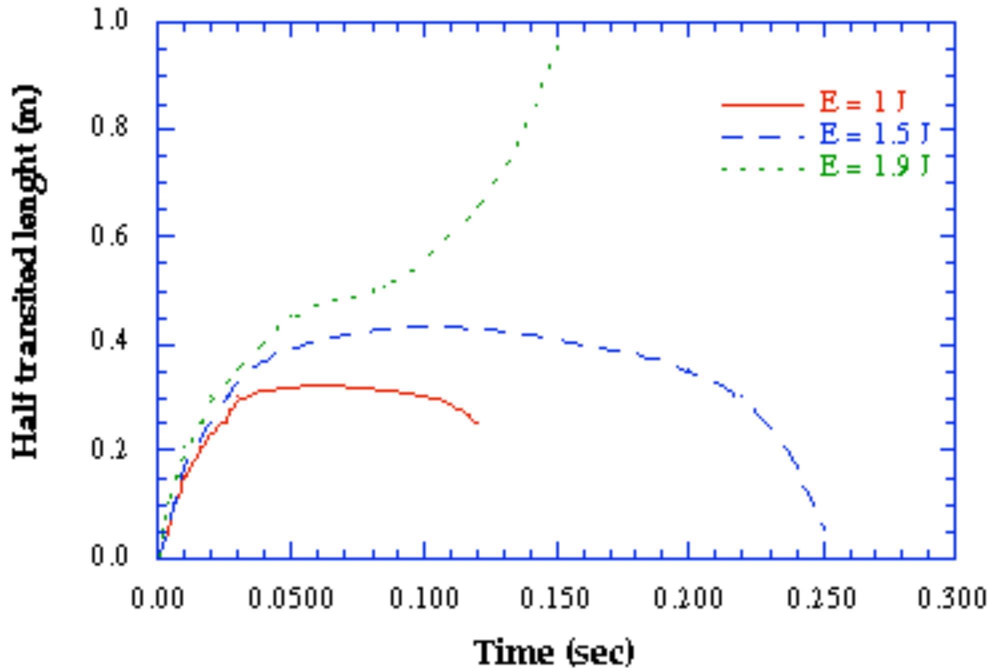

Fig. 15.7: Time evolution of the normal zone in the case of finite current diffusion for the ALEPH coil.

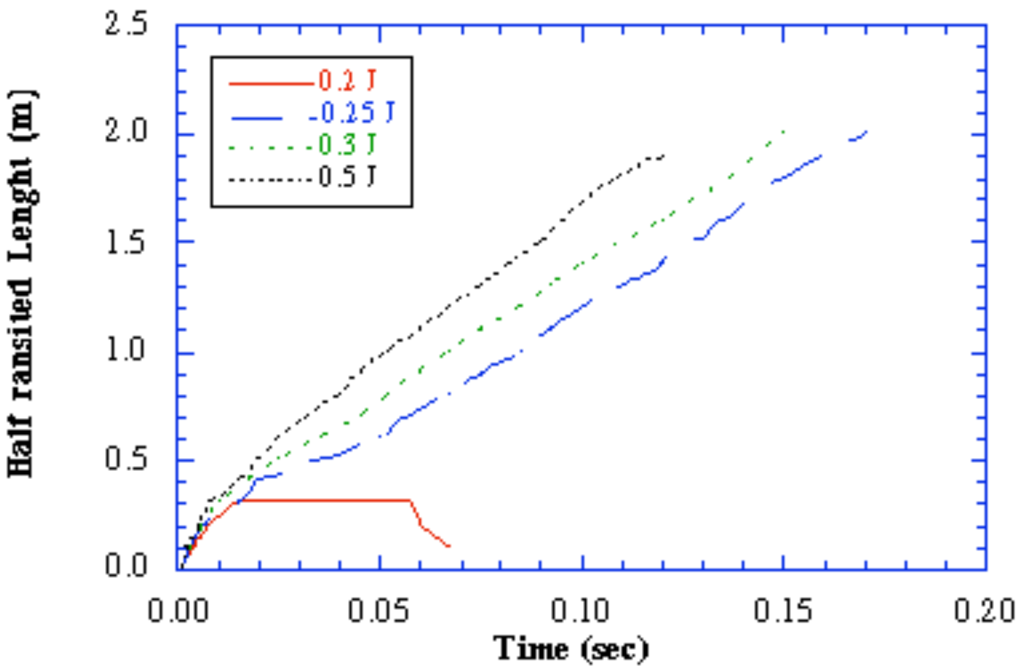

Fig. 15.8: Time evolution of the normal zone in the case of finite current diffusion for CDF coil.

Time t = 0 is defined as the starting time of the disturbance. The disturbance energy is used as a parameter.

Several interesting considerations can be made looking at these results:

a) For both cases there exists a threshold energy at the border between propagation and recovery behaviours. This energy, which we will call Quench Energy, stays between 15 and 16 J in the case of the instantaneous current diffusion and between 1.4 and 1.5 J in the more realistic case of finite current diffusion. Similar analyses on different magnets confirmed that the energy release, dividing propagation from recovery, really stays in a very narrow range, as shown in Fig. 15.7 and 15.8 for ALEPH and CDF.

b) At initial times the transited length grows in the same way for every value of the energy disturbance. The initial growth is followed by a stop of the normal zone propagation if the energy release is less than the Quench Energy. For CMS the propagation stops in a time of 100 ms for the instantaneous current diffusion case and 15 ms in the other case. The quenched zone is stable for some time, and then decays up to a point where the superconductivity is restored. The quenched zone, after the initial growth, continues to grow with a different velocity, if the energy release is close to, but higher than the QE. A possible interpretation could be as follows. The localised disturbance generates a normal region which rapidly grows up to a fixed length (70 cm in the instantaneous current diffusion case and 16 cm in the other case). The flat of the curves represents a metastable region where the heat generation is compensated by the thermal conduction. Since the two contributions are not exactly equal, there is a prevalence of one, causing a quench or a recovery. We think that the flat represents a metastable region, which can be considered as analogue of the so called Minimum Propagating Zone, i.e. a normal zone in thermal equilibrium with the surrounding superconducting environment.

c) The effect of the current diffusion strongly affects the stability, reducing by one order of magnitude the available Quench Energy in the ideal case of instantaneous current diffusion.

An important question is related to the meaning of localised disturbance. We computed the Quench Energy Vs the disturbance duration at a fixed value of the disturbance length (1 cm), as shown in Fig. 15.9. Furthermore, the Quench Energy was computed vs. the disturbance length at a fixed value of the disturbance duration (10 ms) as shown in Fig. 15.10.

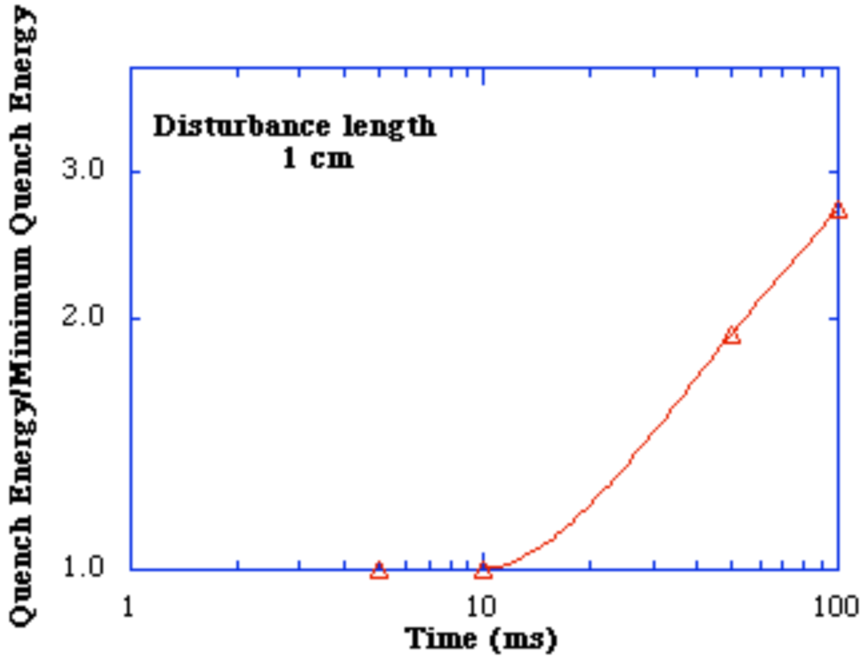

Fig. 15.9: Quench Energy vs. the disturbance duration at a fixed value of the disturbance length (1 cm).

As figures show, the Quench Energy is not depending on the disturbance, for disturbances of lengths up to 3 cm and time durations of up to 10 ms. Since Fig. 15.6 shows that the metastable region (or MPZ) is 16 cm and a time of 15 ms is required to form it, the previous statement is equivalent to saying that the disturbance can be considered localised if its length and duration are respectively smaller (but not necessarily much smaller) than the MPZ length and the time interval to set it. We can define the lowest value of Quench Energy, independent of disturbance length and duration, as the Minimum Quench Energy.

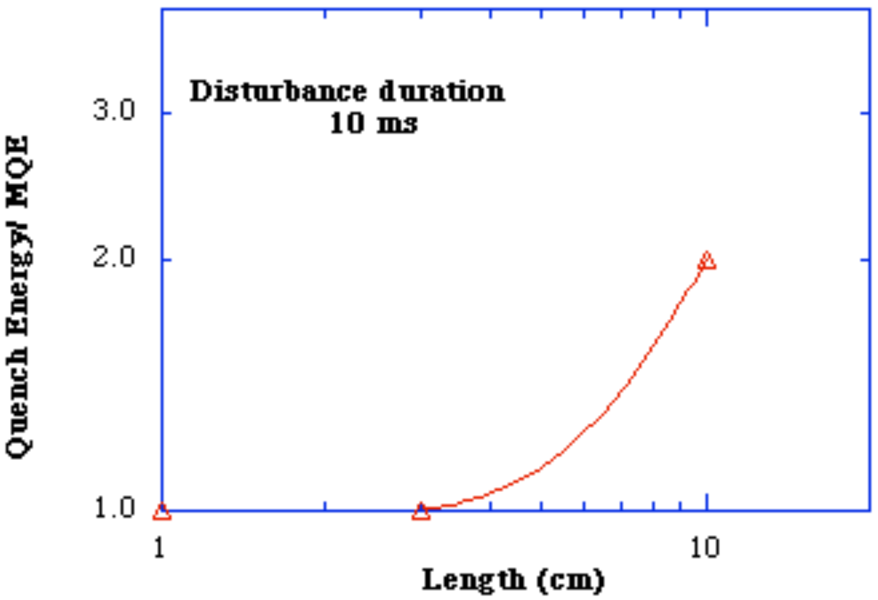

Fig. 15.10: Quench Energy Vs the disturbance length at a fixed value of the disturbance duration (10 ms).

15.4 POSSIBLE DISTURBANCE SOURCES

In this section we briefly analyse the possible heat releases inside the winding, trying to get an idea about the order of magnitude of the released energy or power. The heat releases of a mechanical nature generated directly inside the coil are due to un-reversible phenomena like movements, breakages or slippings, related to basic mechanisms such as stress above the yield limit, shear failure or bonding failure. Though formal and rigorous analysis is a very hard task, some special cases can be analysed.

Pure aluminium in plastic regime

It has been stressed in previous chapters that the hoop force puts the pure aluminium beyond the elastic limit. During a cycle of the magnetic field the energy dissipated per unit volume is given by the integral of the stress over deformation:

$$E = \oint \sigma d\varepsilon \,. \tag{15.6}$$

In our case, this integral, calculated using the curves with 40 MPa yield strength, gives $E = 2.9\ 10^4\ J/m^3$. Considering a total cold mass of pure aluminium of 28 m^3, we have a total dissipation of $8.1\ 10^5$ J. The power generation depends on the charge time as discussed in Chapt. 17. This power can be easily drained away by the cooling circuit with no problems. In this case we have a heat dissipation of mechanical nature, but not strictly related to the coil stability because the phenomenon is in a steady state.

Bonding failure

A bonding failure can occur at several interfaces: Rutherford-pure aluminium, pure aluminium - reinforcement, conductor - insulation, turn to turn, layer to layer. In each case energy could be dissipated. The most dangerous case occurs when the heat is released very close to the Rutherford, so that the cable-pure aluminium bonding must be carefully studied. The mechanical analysis showed that a shear stress of 20 MPa exists at this interface. This shear stress is due to the differential thermal contraction between pure aluminium and the Rutherford cable. Since pure aluminium contracts, from RT. to 4.5 K, much more than Copper and NbTi, the Rutherford is put in compression, while the pure aluminium is in tension. Since the Rutherford is completely surrounded by the pure aluminium, we would also have the same stress if there was no bonding at the interface. As a consequence a failure of this bonding should not be dramatic from the point of view of the release of elastic energy. In case we have an extruded insert, it can be argued that the failure of the bonding could allow micro-movements of the strands under the action of the magnetic field. Looking at typical cross section of Rutherford cable inside pure aluminium, we can observe the existence of voids. The Rutherford is compacted with a filling factor of around 85%. The worst situation happens when under the action of the axial force, one half of the Rutherford moves against the other half. Since the gap between the two halves is s = 0.05 mm, the energy dissipation per unit length is $W = B\ I\ s = 4.3 \cdot 10000 \cdot 5\ 10^{-5} = 2.15$ J/m (we have used a current of 10 kA because only half the Rutherford moves). This energy dissipation is well within the enthalpy margin (4.2 J/m).

Epoxy cracks

Since the epoxy contracts much more than aluminium when cooling down from RT. to 4.5 K, the epoxy is put in tension. The stored elastic energy can be written as :

$$E = \frac{3}{2} Y \varepsilon_0^2 \frac{1}{(1-2\nu)}, \tag{15.7}$$

where Y is the Young's modulus (8 GPa), e_0 is the strain due to the differential contraction (of the order of 8 10^{-3}), n is the Poisson ratio (0.21) and V is the volume. The elastic energy is of the order of 10^6 J/m^3. This energy constitutes a potential disturbance source. Nevertheless in order to have significant disturbances (of the order of the enthalpy margin), a big fraction of epoxy should crack in a large volume. As an example the Enthalpy Margin (4.2 J) is roughly equivalent to the energy stored in the conductor insulation for a length of 25 cm. The complete –insulation crack along 25 cm all around the conductor is quite an improbable occurrence.

15.5 COMPARISON WITH LARGE RUNNING COILS

In the previous sections we discussed the basic concepts to carry out stability transient analyses on an aluminium stabilised superconducting winding. These ideas were preliminary tested by predicting the amount of localised energy necessary to quench a mock up of the DELPHI coil. The predicted values (using 3 different numerical codes HEATING, CASTEM and RALTRAN) and the experimental measurements of MQE ranged within a factor 2. On the basis of these results we think that the developed methods for stability analysis, involving the use of 3D Finite Element Codes, can give realistic information. However if this analysis is applied not only to the magnet under design but also to different (and existing) magnets, one can have comparative results of interest for the design itself.

In this framework we made a comparison of the computed MQE for some aluminium stabilised solenoids with the results obtained for CMS. As for the enthalpy margin the solenoids ALEPH and CDF were considered. In performing comparative studies it is important to consider that the MQE depends on the RRR, which depends on several factors such as the aluminium purity and the stress level in the conductor. Since this information is only partially available, we preferred to compute the MQE for a wide range of values of the RRR at B = 0 T, so that a more general picture about stability is given. The results are shown in Fig. 15.11 and 15.12 for the two cases of instantaneous and finite current diffusion.

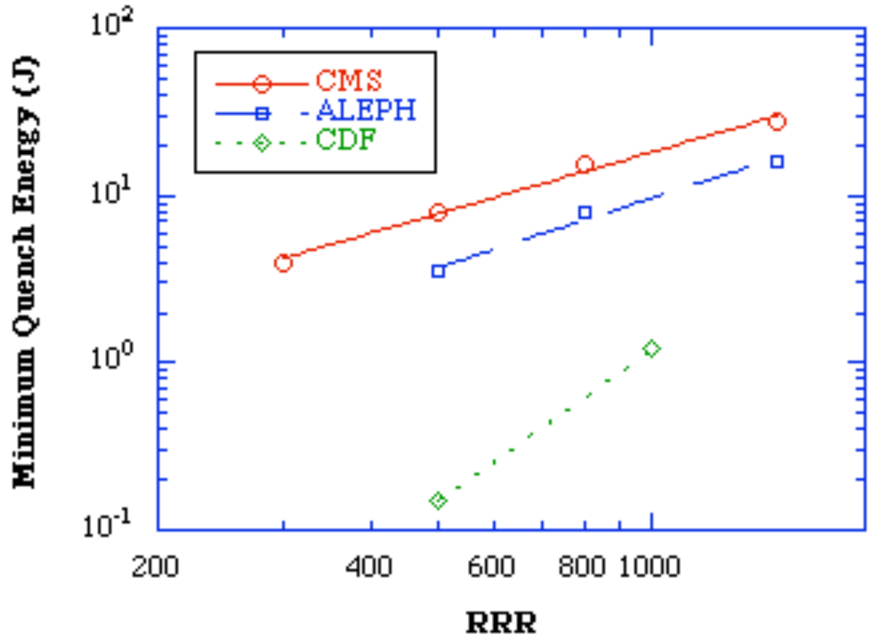

Fig. 15.11: MQE vs. RRR for CMS, CDF and ALEPH solenoids in the case of instantaneous current diffusion.

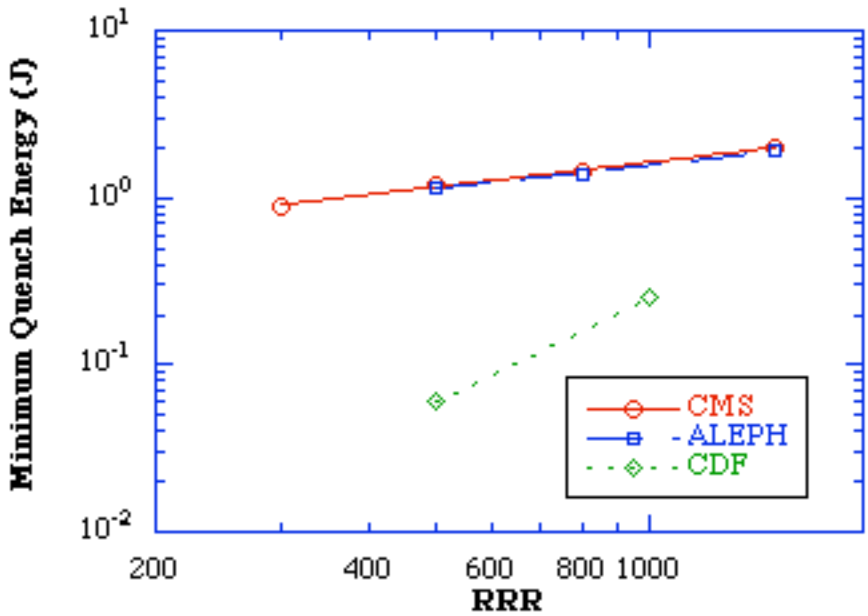

Fig. 15.12: MQE vs. RRR for CMS, CDF and ALEPH solenoids in the case of finite current diffusion.

From the point of view of our interest, i.e. the optimisation of the CMS winding and conductor, we could infer that the stability margin against localised disturbances of CMS is at least of the same order as the ALEPH margin and much higher than the CDF one. Nevertheless a more accurate discussion about this result is needed, because we must relate the calculated stability margin with the level of disturbances.

If we had information about the stress distribution for the three magnets, we should be able to find a correlation between stress (and then possible mechanical disturbances) and stability margins. Since the insulation is the weakest part of the winding, it would be interesting to know the stress distribution in that part.

We carried out this exercise by computing the stress distribution in the insulation of ALEPH and CMS. As parameter for comparison we choose the principal stress S1. Figures 15.13 and 15.14, p. C-42, show a detail of insulation stress in ALEPH and CMS due to the thermal contraction. Fig. 15.15, p. C-43, shows how the CMS insulation stress barely increase due to the magnetic load, as can be seen by looking to Fig. 15.14 which is repeated on the same page to ease comparison.

15.6 CONCLUSIONS

These previous results clearly show that the stresses in insulation are very similar for ALEPH and CMS. They are mainly due to the cool-down from RT. to operating temperature. The potential disturbances for unit volume coming from breaks of insulation or in the epoxy should be the same for both coils.

Since the Enthalpy margin for unit volume and the MQE are similar for both coils, it is possible to conclude that CMS is as stable as ALEPH with respect to localised and distributed disturbances in insulation.